



A Novel Cooperative Teleoperation Framework for Nonlinear Time-Delayed Single-Master/Multi-Slave System

Maryam Farahmandrad[†], Soheil Ganjefar[†], Heidar Ali Talebi[‡] and Mahdi Bayati^{‡*}

[†]Department of Electrical Engineering, Bu-Ali Sina University, Hamedan, Iran. E-mails: m.farahmandrad@alumni.basu.ac.ir, s_ganjefar@basu.ac.ir

[‡]Department of Electrical Engineering, Amirkabir University of Technology. E-mail: alit@aut.ac.ir

(Accepted April 25, 2019. First published online: May 30, 2019)

SUMMARY

This paper proposes a novel control framework for a single-master/multi-slave teleoperation system to grasp and handle an object, considering nonlinearity and uncertainty in the dynamics of the slaves and time-varying delay in the communication channel. Based on passive decomposition approach, the dynamics of the slaves are decomposed into two decoupled systems, and then two higher order sliding mode controllers are designed to control them. Also, a synchronization control methodology for the master is developed. Stability is fully studied using the passivity property and Lyapunov theorem. Finally, simulation and practical results confirm that the control system works well against the conditions.

KEYWORDS: Cooperative robotic system; Higher order sliding mode control; Locked system; Shape system; Single-master/multi-slave; Synchronization control; Teleoperation.

1. Introduction

Teleoperation is used to enable humans to manipulate dangerous, remote, or delicate tasks via robotic manipulators with enhanced safety at lower cost and better accuracy. A teleoperation system includes a master subsystem, which is manipulated by an operator, and some slave subsystems handling the remote environment. They are interconnected via a wireless communication link that may induce time delays on reference signals.¹ These time delays in a closed-loop system can affect the whole stability.² Therefore, in order to accomplish a desired task in a remote environment under communication time delays, each subsystem must have its own local control system to guarantee stability.

Recently, cooperative teleoperation systems have drawn a great deal of attention. In comparison to conventional teleoperation systems, they have big distinct advantages such as better dexterity, improved handling capability, better loading capacity, and enhanced robustness due to redundancy. Hence, they have found vast applications in medical surgery, space station maintenance, and handling large and heavy objects. Depending on the application, there are different formations of master and slaves to form a cooperative teleoperation system. In single-master/multi-slave (SMMS) teleoperation systems, an operator collectively controls multiple slave robots in order to accomplish a common task through a communication channel. Accordingly, a control methodology for facing the challenges is necessary.

Different control methods have been proposed for cooperative systems, and the majority of them such as hybrid position/force control^{3–5} and impedance control⁶ are based on “rigid grip condition.” This term means that the internal grasping shape among the slave robots is maintained rigidly in a

* Corresponding author. E-mail: bayati.mahdi@aut.ac.ir

way. This condition restricts applications of the SMMS systems since the internal grasping shape must be controlled in some applications. This condition is not usually reached unless the objects are rigid and the rigid fixtures are available.⁷ A decentralized adaptive coordinated control method without force sensor for grasping a common object using multiple manipulators has been proposed in ref. [8] in which the rigid contact and the rolling contact between the object and the robots have been analyzed, and it is assumed that the object's center of mass is measurable. Furthermore, a decentralized adaptive and nonadaptive position/force controller for control of cooperative robots has been employed in ref. [9]. Since each robot has been separately controlled, independently of the other robots, load distribution between them is unknown, and thus, this method is not suitable for applications with high precision.

Few studies can be found on "passive decomposition" for handling an object.^{7,10–12} Lee et al. have utilized passive decomposition for bilateral teleoperation between single master and multiple cooperative slave robots in the presence of constant time delays in order to design a control system.^{7,10} In refs. [7, 10], the dynamics of the slaves have been decomposed into two decoupled systems, that is, *locked* and *shape* systems. A Proportional-Integral controller has been developed for the locked system, and a Proportional-Derivative (PD) controller has been developed for the shape system. However, the method is only applicable for point mass mobile robots. In refs. [11, 12], three robot manipulators have been used that their dynamics are supposed to be known. The shaped and locked systems are controlled by two PD controllers in ref. [11], while they are controlled by two Proportional-Integral-Derivative controllers in ref. [12]. In ref. [13], a novel stabilization control framework for a certain class of nonholonomic mechanical systems based on passivity has been proposed. In ref. [14], passive decomposition has been used to design the feed-forward action and the disturbance observer to estimate human force for haptic devices without on-board force sensors. In ref. [15], nonholonomic passive decomposition to split the kinematics of the two wheeled mobile robots into the grasping/first-person view-centering behavior and the teleoperation-related behavior has been used.

There are some other important relevant research studies needed to be discussed in detail. In ref. [16], adaptive control architectures have been developed for SMMS robotic systems in the presence of constant but unknown communication delays. The dynamics of the cooperative system have been expressed based on the measurable point of the object. In ref. [17], an adaptive neural network controller for SMMS teleoperation considering time-varying delays for multiple mobile manipulators carrying a common object in a cooperative manner has been proposed. In ref. [18], a multi-agent system has been applied to a teleoperation system. Moreover, a formation controller for the SMMS teleoperation system with time-varying delays and quantization has been developed. The output signals of the master robot and the slave agents are quantized before transmitting. In ref. [19], a PD controller to enforce position tracking, formation control, force reflection, and collision-free trajectories for an SMMS teleoperation system in the presence of constant time delays has been presented, and finally, the control framework is validated through experimental results.

Additionally, a teleoperation scheme has been presented for a single master and a group of wheeled robots in the presence of constant time delays in ref. [20]. The bilateral teleoperation system includes a haptic device, an overhead camera, and a group of nonholonomic robots. The teleoperation scheme has been implemented and demonstrated in an indoor environment. The proposed algorithm ensures that the robot avoids collision with the neighbor robots and the obstacles in the environment. In ref. [21], the problem of dexterous robotic grasping by means of a telemanipulation system including a single master and two slave manipulators has been presented. In order to achieve a stable rigid grasp, a centralized adaptive force-position controller and a linear velocity observer for the slave robots have been proposed. However, the stability analysis does not consider communication time delays. In ref. [22], design of an SM/MS nonlinear teleoperation system is presented. The communication between the master and slave robots is reached through extended state convergence architecture. Lyapunov–Krasovskii theory is utilized to prove stability and determine the control gains of the teleoperation system. However, the stability analysis does not consider communication time delays. In ref. [23], the formation problem of SM/MS teleoperation system in the presence of the intermittent communications has been proposed. Using small-gain technique, the authors suggest a control scheme achieving formation in the situation where the master and slaves are allowed to communicate with their neighbors only at some irregular discrete time instants. It is shown that the slave robots mimic the movement of the master robot with a desired relative distance.

The purpose of this research study is to control a cooperative teleoperation robotic system which consists of SMMS robots to grasp and handle an object. Using passive decomposition theory, the dynamics of the multiple slave robots are decomposed into two decoupled systems, shape and locked systems, with uncertainty in their dynamics. The reason behind this decision is that secure and tight cooperative grasping can be achieved by locally controlling the decoupled shape system regardless of the communication delay and the human command.⁷ To deal with time-varying delay, uncertainties, and nonlinearities of the cooperative teleoperation system, two control methodologies are proposed for the master and cooperative sides. For the master system, a synchronization control methodology for achieving the desired objective is developed.²⁴ For the cooperative system, two higher order sliding mode controllers (HOSMC) are designed to control the locked system and the shape system. Since classical sliding mode control (SMC) has some intrinsic problems such as chattering phenomenon,²⁵ the HOSMC have been suggested. Additionally, since HOSMC is a robust control technique for nonlinear systems operating under uncertain conditions, it can cope with uncertainty in the dynamics of the shape system and the locked system. The passivity of the closed-loop system is also examined.

The novelty of this paper is that a *comprehensive* scenario has been developed for the cooperative teleoperation system in which *nonlinearity* in the dynamics of the telemanipulators, *uncertainty* in the dynamics of the slave robots, and *time-varying* delay in the communication channel have been considered with the new advanced HOSMC controllers in practice. The proposed control framework would be useful in many significant applications, for instance, where many slave robots are needed to cooperatively manipulate objects with a high grasping precision or where the workplace is located in a remote and uncertain environment so that human intervention is crucial for successful task completion.

The rest of this essay is organized as follows. In Section 2, formulation and modeling of the cooperative teleoperation robotic system are introduced. Passive decomposition is explained in Section 3. Sections 4 and 5 present the control methodology and the stability analysis, respectively. Simulations and experimental results are presented in Sections 6 and 7. Eventually, it finishes with a conclusion in Section 8.

2. Dynamics of SM/MS Teleoperation Systems

A general SMMS robotic system consists of one master with m -DOF and N slave robots with n_i -DOF. Dynamic equation of a robotic system can be expressed as²⁶

$$\begin{cases} M_m(q_m)\ddot{q}_m + C_m(q_m, \dot{q}_m)\dot{q}_m + g_m(q_m) = \tau_m + J_m^T(q_m)F_h, \\ M_i(q_i)\ddot{q}_i + C_i(q_i, \dot{q}_i)\dot{q}_i + g_i(q_i) = \tau_i + J_i^T(q_i)F_i, \end{cases} \quad (1)$$

where the subscript m denotes the master and the subscript $i = 1, \dots, N$ denotes the slaves; $q_m \in R^{m \times 1}$ and $q_i \in R^{n_i \times 1}$ are the joint angle vectors of the robot; $M_m(q_m) \in R^{m \times m}$ and $M_i(q_i) \in R^{n_i \times n_i}$ are the symmetric and positive definite inertia matrices; $C_m(q_m, \dot{q}_m) \in R^{m \times m}$ and $C_i(q_i, \dot{q}_i) \in R^{n_i \times n_i}$ are the matrices of Coriolis and centrifugal forces; $g_m \in R^{m \times 1}$ and $g_i \in R^{n_i \times 1}$ are the vectors of gravitational forces; $\tau_m \in R^{m \times 1}$ and $\tau_i \in R^{n_i \times 1}$ are the control generalized force to be designed; $F_h \in R^{m \times 1}$ is the operational force vector and $F_i \in R^{n_i \times 1}$ is the external force vectors; and $J_m \in R^{m \times m}$ and $J_i \in R^{n_i \times n_i}$ are Jacobian matrices. Important properties of the dynamic equation of (1) can be stated as follows:²⁶

- Property 1
For a manipulator with revolute joints, the inertia matrices $M_m(q_m)$ and $M_i(q_i)$ are symmetric positive-definite for all $q_m \in R^{m \times 1}$ and $q_i \in R^{n_i \times 1}$.
- Property 2
The matrices $\dot{M}_m(q_m) - 2C_m(q_m, \dot{q}_m)$ and $\dot{M}_i(q_i) - 2C_i(q_i, \dot{q}_i)$ are skew-symmetric. Thus, $\dot{q}_m^T(\dot{M}_m(q_m) - 2C_m(q_m, \dot{q}_m))\dot{q}_m = 0$ and $\dot{q}_i^T(\dot{M}_i(q_i) - 2C_i(q_i, \dot{q}_i))\dot{q}_i = 0$ for all $q_m, \dot{q}_m \in R^{m \times 1}$ and $q_i, \dot{q}_i \in R^{n_i \times 1}$.

Since grasping an object and tracking a desired trajectory can be performed in the task space, the master and slave robot dynamics are written directly in it as:

$$\dot{X}_k = J_k(q_k)\dot{q}_k, \quad k = m, i. \quad (2)$$

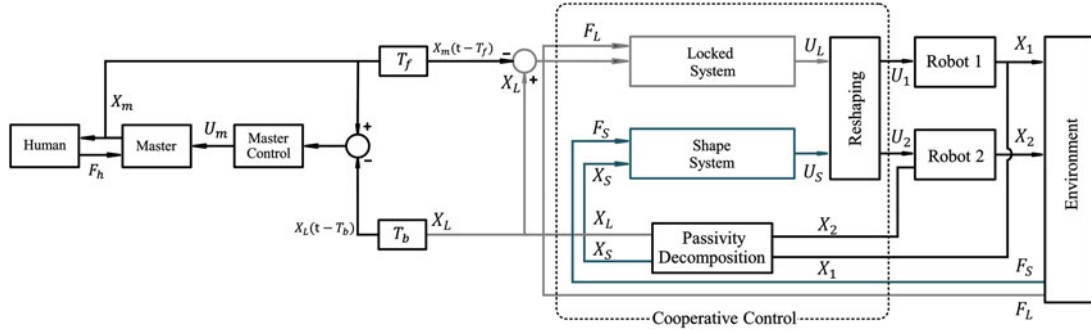


Fig. 1. Shape and locked systems in the cooperative teleoperation system.

After further differentiation of (2), \ddot{X}_k is written as

$$\ddot{X}_k = J_k(q_k)\ddot{q}_k + \dot{J}_k(q_k)\dot{q}_k, \quad k = m, i, \tag{3}$$

where $\dot{X}_m, \ddot{X}_m \in R^{m \times 1}$ and $\dot{X}_i, \ddot{X}_i \in R^{n_i \times 1}$ are the end-effector velocity and acceleration vectors, respectively. Substituting (2) and (3) into (1), the dynamics can be written as follows:

$$\begin{cases} M_{xm}(X_m)\ddot{X}_m + C_{xm}(X_m, \dot{X}_m)\dot{X}_m + G_{xm}(X_m) = U_m + F_h, \\ M_{xi}(X_i)\ddot{X}_i + C_{xi}(X_i, \dot{X}_i)\dot{X}_i + G_{xi}(X_i) = U_i + F_i, \end{cases} \tag{4}$$

where $U_k = J_k^{-T}(q_k)\tau_k$, X_k ($k = m, i$) is the vector of the task space coordinates. Also,

$$\begin{aligned} M_{xk}(X_k) &= J_k^{-T}(q_k)M_k(q_k)J_k^{-1}(q_k), \\ C_{xk}(X_k, \dot{X}_k) &= J_k^{-T}(q_k)(C_k(q_k, \dot{q}_k) - M_k(q_k)J_k^{-1}(q_k)\dot{J}_k(q_k))J_k^{-1}(q_k), \\ G_{xk}(X_k) &= J_k^{-T}(q_k)g_k(q_k). \end{aligned}$$

$n = \sum_i^N n_i$ denotes the total degree of freedom of the N slave robots. Hence, the group dynamics of the N slave robots in the task space can be expressed as

$$M_x(X)\ddot{X} + C_x(X, \dot{X})\dot{X} + G_x(X) = U + F, \tag{5}$$

where

$$\begin{aligned} X &= [X_1^T, \dots, X_N^T]^T \in R^{n \times 1}, \\ U &= [U_1^T, \dots, U_N^T]^T \in R^{n \times 1}, \\ F &= [F_1^T, \dots, F_N^T]^T \in R^{n \times 1}, \\ M_x &= \text{diag}[M_{x1}, \dots, M_{xN}] \in R^{n \times n}, \\ C_x &= \text{diag}[C_{x1}, \dots, C_{xN}] \in R^{n \times n}, \\ G_x &= [G_{x1}^T, \dots, G_{xN}^T]^T \in R^{n \times 1}. \end{aligned}$$

According to the properties 1 and 2, $M_x(X)$ is symmetric and positive-definite. Also, $\dot{M}_x(X) - 2C_x(X, \dot{X})$ is skew-symmetric.²⁶

3. Passive Decomposition

In this section, based on passive decomposition introduced in ref. [27], the n -DOF dynamics of the multiple slave robots in (5) are decomposed into two decoupled systems: the $(n-m)$ -DOF shape system describing the coordination aspect (e.g., the internal group formation of the multiple robots) and the m -DOF locked system describing the overall motion of the robots and the grasped object. Shape and locked system coordinates are defined by X_S and X_L , respectively (see Fig. 1). The grasping shape function (X_S) is defined by relative position of the robots' end effectors as

$$X_S = \begin{pmatrix} X_1 - X_2 \\ \vdots \\ X_{N-1} - X_N \end{pmatrix}, \tag{6}$$

and also, X_L is the average of the robots coordinates.

Considering the tangent-space decomposition in ref. [28], the velocity of the group dynamics (5) can be decomposed into the locked system velocity $\dot{X}_L \in R^m$ and the shape system velocity $\dot{X}_S \in R^{n-m}$ such that

$$\begin{pmatrix} \dot{X}_L \\ \dot{X}_S \end{pmatrix} = \underbrace{\begin{pmatrix} \Psi_1(X) & \Psi_2(X) & \dots & \Psi_N(X) \\ I & -I & \dots & 0 \\ \vdots & \vdots & \ddots & \vdots \\ 0 & 0 & \dots & -I \end{pmatrix}}_{=:S(X) \in R^{n \times n}} \begin{pmatrix} \dot{X}_1 \\ \dot{X}_2 \\ \vdots \\ \dot{X}_N \end{pmatrix}, \tag{7}$$

where $\Psi_i(X)$, ($i = 1, \dots, N$) is given by

$$\Psi_i(X) = [M_{x1}(X_1) + M_{x2}(X_2) + \dots + M_{xN}(X_N)]^{-1} M_{xi}(X_i). \tag{8}$$

Using the fact that $\Psi_i(X)$ in (8) is nonsingular and the following property:

$$\Psi_1(X) + \Psi_2(X) + \dots + \Psi_N(X) = I, \tag{9}$$

we can show that $S(X)$ is nonsingular. Since it is assumed that the two robots are utilized to grasp a rigid object, (7) can be simplified to the following form:

$$\begin{pmatrix} \dot{X}_L \\ \dot{X}_S \end{pmatrix} = \begin{bmatrix} \Psi_1(X) & \Psi_2(X) \\ I & -I \end{bmatrix} \begin{pmatrix} \dot{X}_1 \\ \dot{X}_2 \end{pmatrix}. \tag{10}$$

After decomposition in (10), the group inertia of (5) is now block-diagonalized such that

$$S^{-T}(X)M_x(X)S^{-1}(X) = \begin{bmatrix} M_L(X) & 0 \\ 0 & M_S(X) \end{bmatrix}, \tag{11}$$

where $M_L(X)$ and $M_S(X)$ are symmetric and positive definite inertia matrices for the locked system and the shape system, respectively. We also define compatible decompositions of (10) as

$$\begin{pmatrix} U_L \\ U_S \end{pmatrix} = S^{-T} \begin{pmatrix} U_1 \\ U_2 \end{pmatrix}, \quad \begin{pmatrix} F_L \\ F_S \end{pmatrix} = S^{-T} \begin{pmatrix} F_1 \\ F_2 \end{pmatrix}, \tag{12}$$

$$S^{-T}M_x \frac{d}{dt}(S^{-1}) + S^{-T}C_x S^{-1} = \begin{bmatrix} C_L & C_{LS} \\ C_{SL} & C_S \end{bmatrix}. \tag{13}$$

Then, using (10), the group dynamics of (5) can be decoupled as follows:

$$\underbrace{M_L(X)\ddot{X}_L + C_L(X, \dot{X})\dot{X}_L + G_L}_{\text{Locked system dynamics}} + \underbrace{C_{LS}(X, \dot{X})\dot{X}_S}_{\text{Coupling}} = U_L + F_L, \tag{14}$$

$$\underbrace{M_S(X)\ddot{X}_S + C_S(X, \dot{X})\dot{X}_S + G_S}_{\text{Shape system dynamics}} + \underbrace{C_{SL}(X, \dot{X})\dot{X}_L}_{\text{Coupling}} = U_S + F_S, \tag{15}$$

where $C_L(X, \dot{X})$ and $C_S(X, \dot{X})$ are locked and shape Coriolis matrices. U_L and U_S are the applied forces to the locked system and the shape system. F_L and F_S are the environmental forces affecting the overall robots motion and the internal grasping force, respectively. G_L and G_S are the locked and shape vectors of the gravitational forces.

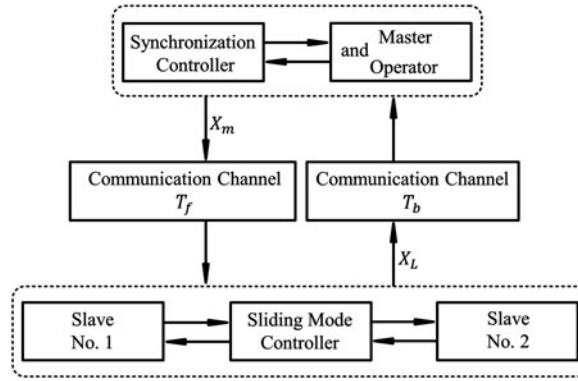


Fig. 2. Block diagram of the delayed cooperative teleoperation system.

• Property 3

The decomposed dynamics (14) and (15) have the following properties⁴:

1. $M_L(X)$ and $M_S(X)$ are symmetric and positive definite.
2. $\dot{M}_L(X) - 2C_L(X, \dot{X})$ and $\dot{M}_S(X) - 2C_S(X, \dot{X})$ are skew-symmetric.
3. $C_{LS}(X, \dot{X}) + C_{SL}^T(X, \dot{X}) = 0$.
4. The kinetic energy and the total environmental/control supply rates are decomposed into sum of those of the locked and the shape systems.

4. Control Methodology

The purpose of the control signals is to coordinate the object through manipulating the master far from the slave environment as well as providing a tele-presence feeling for the human operator. Communication time delays can destabilize an SMMS teleoperation system. Therefore, a control methodology by which the closed-loop stability is guaranteed is required. For this purpose, a synchronization controller is designed for the master and two HOSMCs are designed for the cooperative system (i.e., the shape and the locked systems). Figure 2 depicts the block diagram of such a delayed cooperative teleoperation system.

4.1. Master control

e_m denotes the position error vectors and is defined as

$$e_m = X_m - X_L(t - T_b), \tag{16}$$

where T_b is the time-varying delay. The control objective is to drive the coordination errors e_m to zero. In order to achieve such an objective, the following synchronization signal is proposed:

$$\dot{X}_{mr} = \dot{X}_m + \lambda e_m, \tag{17}$$

where λ is the positive diagonal matrix. After differentiating (17) and substituting the tracking error into the differentiation result,

$$\ddot{X}_{mr} = \ddot{X}_m + \lambda(\dot{X}_m - (1 - \dot{T}_b)\dot{X}_L(t - T_b)). \tag{18}$$

After some algebraic manipulations, the dynamic equation of motion of the master is rewritten based on the synchronization signal \dot{X}_{mr} :

$$M_m(X_m)(\ddot{X}_{mr}) + C_m(X_m, \dot{X}_m)(\dot{X}_{mr}) + \Upsilon_m(X_m, e_m, \dot{e}_m) = U_m + F_h, \tag{19}$$

where

$$\Upsilon_m(X_m, e_m, \dot{e}_m) = M_m(X_m)(-\lambda\dot{e}_m) + C_m(X_m, \dot{X}_m)(-\lambda e_m) + G_m. \tag{20}$$

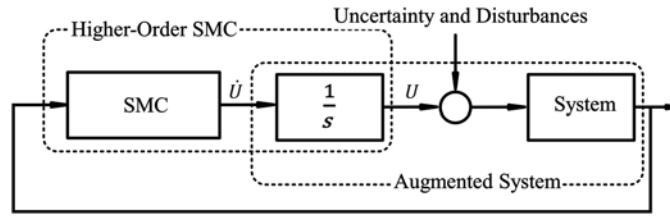


Fig. 3. Higher order sliding mode structure.

In order to achieve the objective, the following controller is proposed:

$$U_m = M_m(X_m) \left(-\lambda(\dot{X}_m - (1 - \dot{\bar{T}}_b)\dot{X}_L(t - T_b)) \right) + C_m(X_m, \dot{X}_m)(-\lambda e_m) + G_m + \bar{\tau}_m + M_m(X_m)\dot{\bar{T}}_b \psi_m, \tag{21}$$

where

$$\bar{\tau}_m = -K_m(\dot{X}_m + \lambda e_m) = -K_m\dot{X}_{mr}. \tag{22}$$

K_m is the positive diagonal matrix and $|\dot{T}_b| \leq \bar{T}_b$. A new term in the control signal, which is called ψ_m , has been considered. Its value will be obtained in the stability proof. After substituting the control law (21) into (19), the closed-loop dynamics for the master system is obtained as:

$$M_m(X_m)(\ddot{X}_{mr}) + C_m(X_m, \dot{X}_m)(\dot{X}_{mr}) = -K_m\dot{X}_{mr} + F_h + M_m(X_m)\dot{\bar{T}}_b \psi_m - M_m(X_m)\dot{X}_L(t - T_b)(\dot{\bar{T}}_b - \dot{T}_b). \tag{23}$$

4.2. Coordination control

The SMC problem for the nonlinear system defined in (14) and (15) is to design the control laws U_L and U_S such that the final closed-loop system is stable and follows a desired position for all possible values of uncertainty in the robot dynamics. SMC theory is extensively utilized due to its attractive features such as good robustness, good transient performance, and fast response. The tracking control problem can be achieved through keeping the system trajectory on the sliding surface $s(t) = 0$.

The sliding surface of classical SMC for a second-order nonlinear systems has the following form:

$$s(t) = \left(\frac{d}{dt} + \lambda \right)^{k-1} e, \tag{24}$$

where k is the relative degree of the system and e is the tracking error. As previously mentioned, the major drawback of SMC is the chattering phenomenon. To avoid this problem and to overcome uncertainty in the robot dynamics, higher order SMC scheme for the locked and the shape systems is proposed. In the second-order SMC, since the time derivative of the control input is defined, the degree of the system is increased to $k + 1$. Therefore, the sliding surface will be changed to

$$s(t) = \left(\frac{d}{dt} + \lambda \right)^k e. \tag{25}$$

The control derivative function appears in the first differentiation of the equation. Since the plant control signal can be considered as the continuous output of a first-order dynamic system like an integrator, this HOSMC does not have noticeable chattering in the control (see Fig. 3).^{29,30}

Two controllers, U_L and U_S (i.e., the control actions for the locked and shape systems, respectively), are designed as follows according to item 3 of property 3:

$$\begin{pmatrix} U_L \\ U_S \end{pmatrix} = \begin{pmatrix} C_{LS}(X, \dot{X})\dot{X}_S \\ C_{SL}(X, \dot{X})\dot{X}_L \end{pmatrix} + \begin{pmatrix} T_L \\ T_S \end{pmatrix}, \tag{26}$$

$$\dot{X}_L^T C_{LS}(X, \dot{X})\dot{X}_S + \dot{X}_S^T C_{SL}(X, \dot{X})\dot{X}_L = 0.$$

This equality with item 4 of property 3 implies that the decoupling procedure does not generate or dissipate any mechanical power. As a result of decoupling in (26), the shape and the locked system dynamics can be expressed as

$$M_L(X)\ddot{X}_L + C_L(X, \dot{X})\dot{X}_L + G_L = T_L + F_L, \tag{27}$$

$$M_S(X)\ddot{X}_S + C_S(X, \dot{X})\dot{X}_S + G_S = T_S + F_S. \tag{28}$$

4.2.1. *Control of the locked system.* In this part, the second-order sliding mode controller for the locked system is designed. The switching function s_L for the locked system is defined as follows:

$$s_L = \left(\frac{d}{dt} + \lambda_L \right)^2 e_L = \ddot{e}_L + 2\lambda_L \dot{e}_L + \lambda_L^2 e_L, \tag{29}$$

where $e_L = X_L - X_m(t - T_f)$ is the tracking error of the locked system. Since the time delay between the locked system and the master robot is time-varying, its derivative exists in the derivative of the tracking error of the locked system as:

$$\dot{e}_L = \dot{X}_L - (1 - \dot{T}_f)\dot{X}_m(t - T_f). \tag{30}$$

T_f is the value of the time-varying delay for the forward communication channel from the master system to the cooperative system. λ_L in (29) is a positive diagonal matrix. After differentiating (29) and substituting the tracking error into the differentiation result,

$$\begin{aligned} \dot{s}_L = & \ddot{X}_L - \ddot{X}_m(t - T_f) + \dot{T}_f \ddot{X}_m(t - T_f) + 2\lambda_L(\ddot{X}_L - \ddot{X}_m(t - T_f)) \\ & + 2\lambda_L(\dot{T}_f \dot{X}_m(t - T_f)) + \lambda_L^2(\dot{X}_L - \dot{X}_m(t - T_f)) + \lambda_L^2(\dot{T}_f \dot{X}_m(t - T_f)), \end{aligned} \tag{31}$$

and assuming the uncertainty in the robot dynamics with differentiating the dynamic model for the locked system,

$$\hat{M}_L(X)\ddot{X}_L + \hat{M}_L(X)\ddot{X}_L + \hat{C}_L(X, \dot{X})\dot{X}_L + \hat{C}_L(X, \dot{X})\dot{X}_L + \hat{G}_L = \dot{T}_L + \dot{F}_L. \tag{32}$$

Now, assume that the upper bound on the rate of changes in the time delay is known ($|\dot{T}_f| \leq \bar{T}_f$). Second-order SMC increases the system degree to one more. Therefore, there is no need to know the time delay of the communication channel. In fact, the control signal requires only the upper bound of the first derivative of the time delay which is not actually a tight limit. It is possible to predict the upper bound of the time delay and its derivatives according to ref. [31]. SMC law for the locked system is proposed as follows:

$$\begin{aligned} \dot{T}_L = & M_L \left(\left(1 - \bar{T}_f \right) \ddot{X}_m(t - T_f) - 2\lambda_L(\ddot{X}_L - \ddot{X}_m(t - T_f)) - \lambda_L^2(\dot{X}_L - \dot{X}_m(t - T_f)) \right) \\ & - 2\lambda_L(\bar{T}_f \ddot{X}_m(t - T_f)) - \lambda_L^2(\bar{T}_f \dot{X}_m(t - T_f)) + (C_L + C_L^T)\ddot{X}_L \\ & + C_L(\ddot{X}_m(t - T_f) - 2\lambda_L \dot{e}_L - \lambda_L^2 e_L) + \dot{C}_L \dot{X}_L + \dot{G}_L - \dot{F}_L - k_L \text{sign}(s_L) + \bar{T}_f M_L \dot{\psi}_L, \end{aligned} \tag{33}$$

where k_L is a positive diagonal matrix and it is assumed that F_L is measured accurately. In the control signal, a new term which is called $\dot{\psi}_L$ has been considered. Its value will be obtained in the stability proof. After substituting (33) into (32), the closed-loop dynamics for the locked system is obtained as

$$\begin{aligned} M_L(X)\dot{s}_L + C_L(X, \dot{X})s_L + k_L \text{sign}(s_L) = & -\phi_L \\ & - M_L(X) \left(\bar{T}_f - \dot{T}_f \right) \left(\ddot{X}_m(t - T_f) + 2\lambda_L \dot{X}_m(t - T_f) + \lambda_L^2 X_m(t - T_f) \right) + \bar{T}_f M_L(X) \dot{\psi}_L. \end{aligned} \tag{34}$$

$\phi_L = [\phi_{L1} \ \phi_{L2}]^T$, $|\phi_{Lj}| \leq \xi_{Lj}$ is defined as the upper bound of the uncertainty. Also, ξ_{Lj} is a bounded positive constant.

4.2.2. *Control of the shape system.* To provide a safe and smooth grasping, an HOSMC is proposed for the shape system. The control objective of the shape system is $X_S \rightarrow X_S^d$ where $X_S^d \in R^{n-m}$ is

a constant desired grasping shape that can be time-varying. Using a similar approach, the sliding surface, the dynamic model, and the control signal T_S for the shape system can be obtained as follows:

$$s_S = \left(\frac{d}{dt} + \lambda_S\right)^2 e_S = \ddot{e}_S + 2\lambda_S \dot{e}_S + \lambda_S^2 e_S, \tag{35}$$

$$\dot{s}_S = \ddot{e}_S + 2\lambda_S \dot{e}_S + \lambda_S^2 e_S = (\ddot{X}_S - \ddot{X}_S^d) + 2\lambda_S(\dot{X}_S - \dot{X}_S^d) + \lambda_S^2(X_S - X_S^d) = 0, \tag{36}$$

where $e_S = X_S - X_S^d$ is the tracking error of the shape system and λ_S is a positive diagonal matrix. X_S^d can be time-varying. Each robotic system has a particular duty. Therefore, X_S^d must be determined with respect to its particular duty and, in turn, a particular shape is reached. However, we confine our attention to a constant X_S^d for brevity. Cooperative grasping can be achieved by locally controlling the decoupled shape system regardless of the communication delay and the human command. So, the time delay has no effect on the tracking error of the shape system and its derivatives,

$$\dot{e}_S = \dot{X}_S - \dot{X}_S^d. \tag{37}$$

Also,

$$\dot{M}_S(X)\ddot{X}_S + \hat{M}_S(X)\ddot{X}_S + \hat{C}_S(X, \dot{X})\dot{X}_S + \hat{C}_S(X, \dot{X})\ddot{X}_S + \hat{G}_S = \dot{T}_S + \dot{F}_S, \tag{38}$$

$$\begin{aligned} \dot{T}_S = & M_S(\ddot{X}_S^d - 2\lambda_S \dot{e}_S - \lambda_S^2 e_S) + (C_S + C_S^T)\ddot{X}_S \\ & + C_S(\ddot{X}_S^d - 2\lambda_S \dot{e}_S - \lambda_S^2 e_S) + \dot{C}_S \dot{X}_S + \dot{G}_S - \dot{F}_S - k_S \text{sign}(s_S). \end{aligned} \tag{39}$$

The closed-loop dynamics for the shape system is

$$M_S \dot{s}_S + C_S s_S = -\phi_S - k_S \text{sign}(s_S), \tag{40}$$

where ϕ_S is defined the same as that for the locked system.

5. Stability Analysis

This section discusses stability analysis for the proposed SMMS system in the presence of the communication time-varying delays. Also, the new terms in the control signals (21) and (33) will be achieved.

• *Theorem*

Consider that the master system (19) is controlled by the synchronization control law. Also, the locked system (32) and the shape system (38) are controlled by the higher order SMC laws. Then, the signals \dot{X}_{mr} , s_L , and s_S are bounded. Moreover, the position tracking errors asymptotically converge to zero for any bounded time-varying delay with a known upper bound on the rate of changes in the time delay. Consider the human operator is passive with $\dot{X}_{mr}(t)$ as the output and $F_h(t)$. Thus, there is a constant value, $k_h \in R^+$, such that

$$-\int_0^t F_h^T(\sigma) \dot{X}_{mr}(\sigma) d\sigma \geq -k_h. \tag{41}$$

• *Proof*

Consider Lyapunov's function candidate as

$$V = V_m + V_L + V_S, \tag{42}$$

where V_m , V_L , and V_S are given by

$$V_m = \frac{1}{2} \dot{X}_{mr}^T M_m \dot{X}_{mr} + \int_0^t -F_h^T(\sigma) \dot{X}_{mr}(\sigma) d\sigma + k_h, \tag{43}$$

$$V_L = \frac{1}{2} s_L^T M_L s_L, \tag{44}$$

$$V_S = \frac{1}{2} s_S^T M_S s_S. \tag{45}$$

The time derivative of V_m is

$$\dot{V}_m = \dot{X}_{mr}^T M_m \ddot{X}_{mr} + \frac{1}{2} \dot{X}_{mr}^T \dot{M}_m \dot{X}_{mr} - F_h^T \dot{X}_{mr}. \tag{46}$$

Using Eq. (19) and the fact that $\dot{M}_m - 2C_m$ is a skew-symmetric matrix, \dot{V}_m is simplified as

$$\begin{aligned} \dot{V}_m &= \dot{X}_{mr}^T \left(-C_m \dot{X}_{mr} - K_m \dot{X}_{mr} + F_h + M_m \dot{\bar{T}}_b \dot{\psi}_m - M_m \dot{X}_L(t - T_b) (\dot{\bar{T}}_b - \dot{T}_b) \right) \\ &\quad + \frac{1}{2} \dot{X}_{mr}^T \dot{M}_m \dot{X}_{mr} - F_h^T \dot{X}_{mr} \\ &= \dot{X}_{mr}^T \left(-C_m \dot{X}_{mr} - K_m \dot{X}_{mr} + F_h + M_m \dot{\bar{T}}_b \dot{\psi}_m - M_m \dot{X}_L(t - T_b) (\dot{\bar{T}}_b - \dot{T}_b) \right) \\ &\quad + \frac{1}{2} \dot{X}_{mr}^T (C_m + C_m^T) \dot{X}_{mr} - F_h^T \dot{X}_{mr}. \end{aligned} \tag{47}$$

After some simplifications, Eq. (47) becomes

$$\begin{aligned} \dot{V}_m &= -\dot{X}_{mr}^T K_m \dot{X}_{mr} + \dot{X}_{mr}^T M_m \dot{\bar{T}}_b \dot{\psi}_m - \dot{X}_{mr}^T M_m \dot{X}_L(t - T_b) (\dot{\bar{T}}_b - \dot{T}_b) \\ &\leq -\dot{X}_{mr}^T K_m \dot{X}_{mr} + \dot{X}_{mr}^T M_m \dot{\bar{T}}_b \dot{\psi}_m - \dot{X}_{mr}^T M_m \dot{\bar{T}}_b \left(1 + \text{sign}(\dot{X}_L(t - T_b)) \right) \dot{X}_L(t - T_b). \end{aligned} \tag{48}$$

According to Eq. (48), it is assumed that $\dot{\psi}_m = \left(1 + \text{sign}(\dot{X}_L(t - T_b)) \right) \dot{X}_L(t - T_b)$. After this assumption and some simplifications,

$$\begin{aligned} \dot{V}_m &= -\dot{X}_{mr}^T K_m \dot{X}_{mr} + \dot{X}_{mr}^T M_m \left(\dot{\bar{T}}_b \text{sign}(\dot{X}_L(t - T_b)) + \dot{T}_b \right) \dot{X}_L(t - T_b) \\ &\leq -\dot{X}_{mr}^T K_m \dot{X}_{mr} \leq 0. \end{aligned} \tag{49}$$

Since K_m is a positive diagonal matrix, it is proved that $\dot{V}_m \leq 0$. The time derivative of V_L is

$$\dot{V}_L = s_L^T M_L \dot{s}_L + \frac{1}{2} s_L^T \dot{M}_L s_L. \tag{50}$$

Using Eq. (34) and the fact that $\dot{M}_L - 2C_L$ is a skew-symmetric matrix, \dot{V}_L is simplified as:

$$\begin{aligned} \dot{V}_L &= s_L^T \left(-C_L s_L - k_L \text{sign}(s_L) - \dot{M}_L \ddot{X}_L - \tilde{M}_L \ddot{X}_L - \dot{\tilde{C}}_L \dot{X}_L - \tilde{C}_L \ddot{X}_L - \dot{\tilde{G}}_L \right. \\ &\quad \left. + \dot{\bar{T}}_f M_L \dot{\psi}_L - M_L (\dot{\bar{T}}_f - \dot{T}_f) (\ddot{X}_m(t - T_f) + 2\lambda_L \ddot{X}_m(t - T_f) + \lambda_L^2 \dot{X}_m(t - T_f)) \right) \\ &+ \frac{1}{2} s_L^T \dot{M}_L s_L = s_L^T \left(-C_L s_L - k_L \text{sign}(s_L) - (\tilde{C}_L + \dot{\tilde{C}}_L^T) \ddot{X}_L - \tilde{M}_L \ddot{X}_L - \dot{\tilde{C}}_L \dot{X}_L - \tilde{C}_L \ddot{X}_L \right. \\ &\quad \left. - \dot{\tilde{G}}_L + \dot{\bar{T}}_f M_L \dot{\psi}_L - M_L (\dot{\bar{T}}_f - \dot{T}_f) (\ddot{X}_m(t - T_f) + 2\lambda_L \ddot{X}_m(t - T_f) + \lambda_L^2 \dot{X}_m(t - T_f)) \right) \\ &\quad + \frac{1}{2} s_L^T (C_L + C_L^T) s_L = s_L^T \left(-k_L \text{sign}(s_L) - \phi_L - M_L (\dot{\bar{T}}_f - \dot{T}_f) (\ddot{X}_m(t - T_f) \right. \\ &\quad \left. + 2\lambda_L \ddot{X}_m(t - T_f) + \lambda_L^2 \dot{X}_m(t - T_f)) + \dot{\bar{T}}_f M_L \dot{\psi}_L \right) = -s_L^T k_L \text{sign}(s_L) - s_L^T \phi_L \\ &\quad - s_L^T M_L (\dot{\bar{T}}_f - \dot{T}_f) (\ddot{X}_m(t - T_f) + 2\lambda_L \ddot{X}_m(t - T_f) + \lambda_L^2 \dot{X}_m(t - T_f)) + s_L^T \dot{\bar{T}}_f M_L \dot{\psi}_L. \end{aligned} \tag{51}$$

After some simplifications, Eq. (51) becomes

$$\begin{aligned} \dot{V}_L &= -s_L^T k_L \text{sign}(s_L) - s_L^T \phi_L - s_L^T M_L (\dot{\bar{T}}_f - \dot{T}_f) \left(\ddot{X}_m(t - T_f) + 2\lambda_L \dot{X}_m(t - T_f) \right. \\ &\quad \left. + \lambda_L^2 \dot{X}_m(t - T_f) \right) + s_L^T \dot{\bar{T}}_f M_L \dot{\psi}_L \\ &\leq -s_L^T k_L \text{sign}(s_L) - s_L^T \phi_L + s_L^T \dot{\bar{T}}_f M_L \dot{\psi}_L - s_L^T M_L \dot{\bar{T}}_f \left(1 + \text{sign}(\ddot{X}_m(t - T_f)) \right. \\ &\quad \left. + 2\lambda_L \dot{X}_m(t - T_f) + \lambda_L^2 \dot{X}_m(t - T_f) \right) \left(\ddot{X}_m(t - T_f) + 2\lambda_L \dot{X}_m(t - T_f) + \lambda_L^2 \dot{X}_m(t - T_f) \right). \end{aligned} \quad (52)$$

According to Eq. (52), it is assumed that

$$\begin{aligned} \dot{\psi}_L &= \left(1 + \text{sign}(\ddot{X}_m(t - T_f) + 2\lambda_L \dot{X}_m(t - T_f) + \lambda_L^2 \dot{X}_m(t - T_f)) \right) \\ &\quad \left(\ddot{X}_m(t - T_f) + 2\lambda_L \dot{X}_m(t - T_f) + \lambda_L^2 \dot{X}_m(t - T_f) \right). \end{aligned} \quad (53)$$

After some simplifications,

$$\begin{aligned} \dot{V}_L &= -s_L^T k_L \text{sign}(s_L) - s_L^T \phi_L + s_L^T M_L \left(\dot{\bar{T}}_f \text{sign}(\ddot{X}_m(t - T_f)) \right. \\ &\quad \left. + 2\lambda_L \dot{X}_m(t - T_f) + \lambda_L^2 \dot{X}_m(t - T_f) \right) + \dot{T}_f \left(\ddot{X}_m(t - T_f) + 2\lambda_L \dot{X}_m(t - T_f) \right. \\ &\quad \left. + \lambda_L^2 \dot{X}_m(t - T_f) \right) \leq -s_L^T k_L \text{sign}(s_L) - s_L^T \phi_L. \end{aligned} \quad (54)$$

Then, for $j \in \{1, \dots, m\}$, Eq. (54) becomes

$$\dot{V}_L \leq \sum_{j=1}^m (-k_{Lj} |s_{Lj}| - \phi_{Lj} s_{Lj}). \quad (55)$$

After assuming $|\phi_{Lj}| \leq \xi_{Lj}$ and some simplifications,

$$\dot{V}_L \leq \sum_{j=1}^m (-k_{Lj} |s_{Lj}| + |\phi_{Lj}| |s_{Lj}|) \leq \sum_{j=1}^m (-k_{Lj} |s_{Lj}| + \xi_{Lj} |s_{Lj}|). \quad (56)$$

To converge s_L to zero, \dot{V}_L must be negative. Therefore, k_{Lj} and ξ_{Lj} should be chosen such that the inequality $-k_{Lj} + \xi_{Lj} < 0$ is satisfied. Hence, with regard to this condition, it is proved that $\dot{V}_L \leq 0$. Using the same technique and the inequality $-k_{Sj} + \xi_{Sj} < 0$, the time derivative of V_S can be obtained as

$$\dot{V}_S = \sum_{j=1}^{n-m} (-k_{Sj} |s_{Sj}| - \phi_{Sj} s_{Sj}) \leq 0. \quad (57)$$

Therefore, \dot{V} can be simplified as

$$\dot{V} = \dot{V}_m + \dot{V}_L + \dot{V}_S \leq -\dot{X}_{mr}^T K_m \dot{X}_{mr} + \sum_{i \in \{L, S\}} [-s_i^T k_i \text{sign}(s_i) - s_i^T \phi_i] \leq 0. \quad (58)$$

After integrating Eq. (41) and using the inequality $-k_{ij} + \xi_{ij} < 0$, it is easy to find

$$\begin{aligned} \int_0^t \dot{V} = V(t) - V(0) &\leq - \int_0^t \dot{X}_{mr}^T K_m \dot{X}_{mr} \\ &\quad + \left(\int_0^t \left(\sum_{i \in \{L, S\}} [-s_i^T k_i \text{sign}(s_i) - s_i^T \phi_i] \right) \right) \leq 0. \end{aligned} \quad (59)$$

So, we can find $V(t) \leq V(0)$. Considering the fact that $V(t) \geq 0$, $V(t) \leq V(0)$, and $\dot{V}(t) \leq 0$, it is possible to say that $V(t)$ is a positive bounded decreasing function. Thus, it is concluded that all terms in $V(t)$ are bounded. Since all terms in $V(t)$ are bounded, \dot{X}_{mr} and s_i are bounded. Therefore, $\dot{X}_{mr}, s_i \in L_\infty$. Furthermore, according to the definition of the sliding surfaces, it is concluded that $e_L, e_S \in L_\infty$. As a result, all the variables of (29) and (35) are bounded. In other words, $\dot{s}_i \in L_\infty$. According to Corollary of Barbalat's Lemma, $\lim_{t \rightarrow \infty} |s_i| = 0$. It is concluded that e_L and e_S asymptotically converge to zero, $\lim_{t \rightarrow \infty} e_L, e_S \rightarrow 0$. On the other hand, according to the definition given in Eq. (17) for \dot{X}_{mr} and using the boundedness of this parameter ($\dot{X}_{mr} \in L_\infty$), it is concluded that \dot{X}_m and e_m are bounded ($\dot{X}_m, e_m \in L_\infty$). All the variables of (18) are bounded ($\dot{X}_{mr} \in L_\infty$). Therefore, using Corollary of Barbalat's Lemma again, $\lim_{t \rightarrow \infty} \dot{X}_{mr} = 0$. As previously mentioned, $\lim_{t \rightarrow \infty} e_L \rightarrow 0$. So, it is concluded that the time derivative of X_m converges to zero, $\lim_{t \rightarrow \infty} \dot{X}_m \rightarrow 0$. Using this result and the fact that $\lim_{t \rightarrow \infty} \dot{X}_{mr} = 0$, it is concluded that e_m asymptotically converges to zero, $\lim_{t \rightarrow \infty} e_m \rightarrow 0$. This completes the proof of the theorem. \square

6. Simulation Results

In this section, the performance of the proposed control scheme is shown by means of simulations on a single master/dual slave system. All the manipulators are similar in the kinematic and dynamic parameters and are modeled as 2-DOF serial link manipulators. The parameters used in the simulations are $m_1 = m_2 = 0.5$ and $l_1 = l_2 = 0.75$, which are the masses and the lengths of the first and the second links, respectively. Moreover, the masses in the robot dynamics are considered with %50 uncertainty as

$$\hat{m}_i = m_i + \Delta m_i, \quad |\Delta m_i| \leq 0.25 \quad i \in \{1, 2\}. \quad (60)$$

It is supposed that two robot manipulators grasp and handle a rigid object with a known shape. Hence, the desired grasp shape can be obtained with respect to the object's shape. The set point for the shape system is considered as

$$X_S^d = [0, 0.3]^T, \quad (61)$$

where 0.3^m is the length of the object that is placed among the two manipulators in Y -direction. The parameter values for the proposed controllers are

$$\begin{aligned} \lambda &= \begin{bmatrix} 1 & 0 \\ 0 & 1 \end{bmatrix}, \\ \lambda_L &= \begin{bmatrix} 15 & 0 \\ 0 & 10 \end{bmatrix}, \\ \lambda_S &= \begin{bmatrix} 20 & 0 \\ 0 & 20 \end{bmatrix}, \\ K_m &= \begin{bmatrix} 2 & 0 \\ 0 & 2 \end{bmatrix}, \\ k_L &= \begin{bmatrix} 600 & 0 \\ 0 & 600 \end{bmatrix}, \\ k_S &= \begin{bmatrix} 300 & 0 \\ 0 & 300 \end{bmatrix}. \end{aligned} \quad (62)$$

The Linear Time-Invariant models of the hand and the environment can be stated as $F_i = F_i^* + Z_e \dot{X}_i$ and $F_h = F_h^* - Z_h \dot{X}_m$, where F_h^* and F_i^* are the external forces exerted by the human operator and the environment on the end-effectors of the master and slave robots, respectively. Z_h and Z_e are the operator's hand impedance and the environment impedance, respectively. Since it is assumed that the environment is passive in our structure, F_i^* in the above equation will be equal to zero. So, the

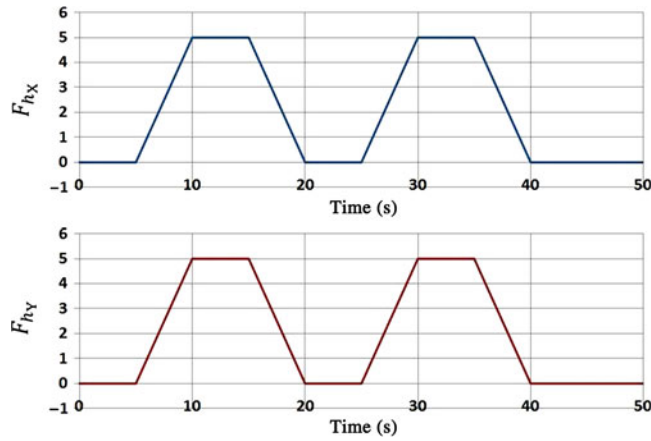


Fig. 4. The operator’s external force in X and Y directions

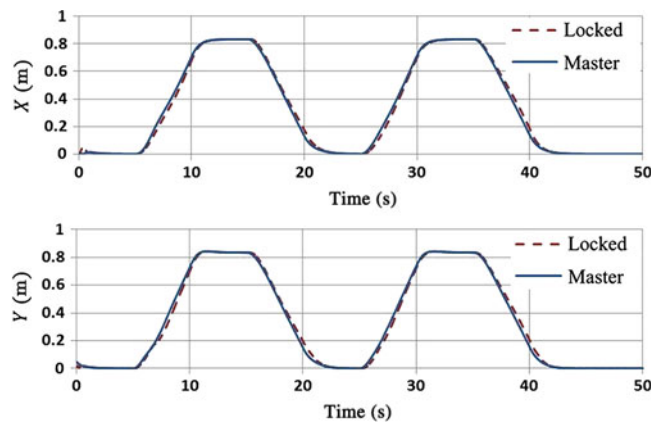


Fig. 5. Position of the master and the locked systems in the presence of the time-varying delay.

object is considered as a mass-spring-damper model which generates the environmental forces. The round-trip time-varying delay in the communication channel is

$$\begin{aligned}
 T_f &= 0.1 \sin(t) + 0.2, \\
 T_b &= 0.1 \sin(t) + 0.15.
 \end{aligned}
 \tag{63}$$

We aim to find the control signal T_L , and thus all its terms must be known. To find the acceleration vector, differentiators to take the derivatives of the position vector have been used. $\dot{\psi}_L$ has appeared in the derivative of the control signal \dot{T}_L (see the term $\dot{\bar{T}}_f M_L \dot{\psi}_L$ in Eq. (33) and also, Eq. (53)). There is no need to calculate the third derivative of the position vector for the control signal T_L because T_L does not include $\ddot{X}_m(t - T_f)$. \dot{T}_L includes $\ddot{X}_m(t - T_f)$ and T_L includes $\int M_L \ddot{X}_m(t - T_f)$. To find it, *integration by parts* formula in mathematics can be used. Therefore,

$$\begin{aligned}
 \int M_L \ddot{X}_m(t - T_f) &= M_L \dot{X}_m(t - T_f) - \int \dot{M}_L \dot{X}_m(t - T_f) dt \\
 &= M_L \dot{X}_m(t - T_f) - \int (C_L + C_L^T) \dot{X}_m(t - T_f) dt.
 \end{aligned}
 \tag{64}$$

The bounded forces exerted on the master robot from the operator is shown in Fig. 4. The simulation results for the single master/dual slave system are shown in Figs. 5–11. Figure 5 shows the time responses of the end-effector position of the locked system with the master in the X–Y plane. As clearly shown, the locked system accurately tracks the master position. Figure 6 depicts the shape system that have reached the desired position in a short time. Figures 7 and 8 show the locked and

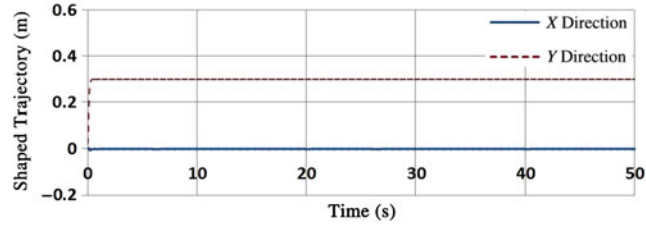


Fig. 6. Trajectory tracking of the shape system.

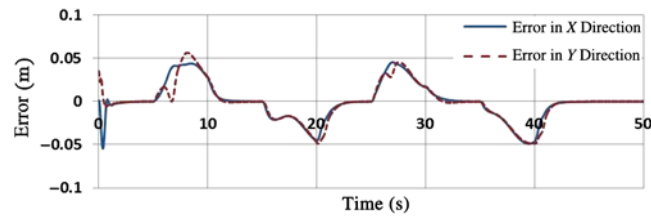


Fig. 7. Trajectory tracking error of the locked system.

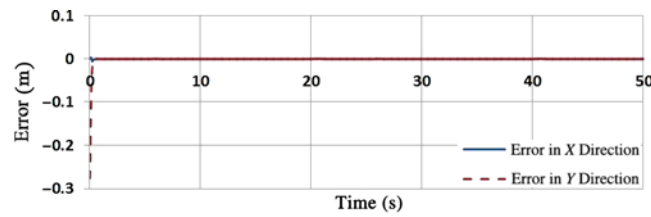


Fig. 8. Grasping shape error.

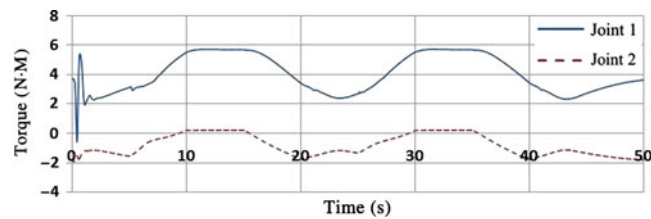


Fig. 9. Control torque of the master robot joints.

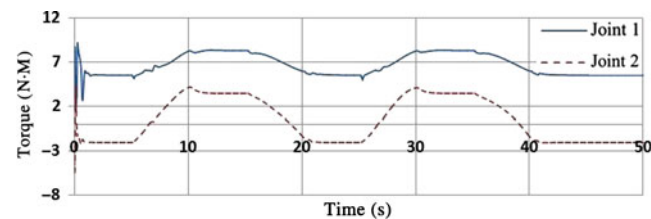


Fig. 10. Control torque of the first robot joints.

the shape tracking errors, respectively. As shown in these figures, the trajectory tracking error of the shape and the locked systems rapidly converge to zero. Figure 9 illustrates the control signal of the master. Finally, Figs. 10 and 11 depict the control signals of the first and the second slave robots, respectively. There is no chattering in the control signals. They are smooth because the HOSMCs have been employed. The simulation results reveal perfect trajectory tracking in the task space with the time-varying communication delays for the shape and the locked systems.

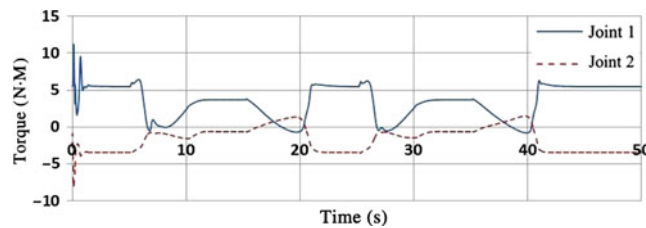


Fig. 11. Control torque of the second robot joints.



Fig. 12. Phantom Omni haptic device.

7. Experimental Study

The proposed control methodology has been implemented for a surgical robot at Realtime Systems Lab at Amirkabir University of Technology. The first part concerns the experimental setup and the other one represents the experimental results.

7.1. Experimental setup

The experimental setup of the teleoperation system can be separated into two parts, Phantom Omni shown in Fig. 12 as the master side and 4-DOF RRPR surgical manipulator shown in Fig. 13 as the slave side. The surgical manipulators have four links. The purpose of the manipulator is to be employed as a surgical tool for beating heart surgery. Position tracking problem is considered in the X–Y–Z directions. The dynamics of the robots are written in the task space. Additionally, the master side is Phantom Omni device that helps the operator to command the position and the orientations to the slaves in the 3D space feedback. The main loop is controlled through Matlab/Simulink and Real-Time Windows Target.

7.2. Experimental results

One degree of freedom is considered and a sponge with size of 10 centimeters has been selected as the object. Thus, the set point for the shape system can be expressed as:

$$X_S^d = [0.1, 0.05].$$

The variable delay is modeled in Simulink environment as

$$T = 0.2 + 0.2 \sin(t).$$

Figures 14 and 15 illustrate the experimental results. Figure 14 depicts tracking the position for the locked system. It reveals that the new method has suitable position tracking in the presence of the time-varying delay. As clearly shown, the locked system accurately tracks the position of the master system. Figure 15 depicts tracking the position for the shape system in terms of two directions,



Fig. 13. 4-DOF RRPR surgical manipulator.

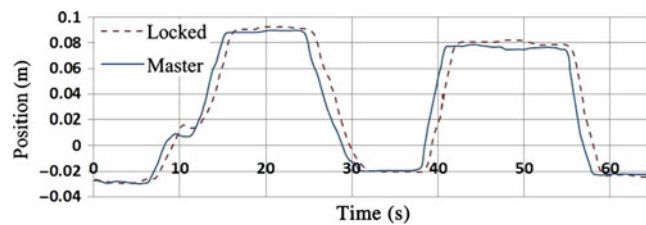


Fig. 14. Position of the master and the locked systems in the presence of the time-varying delay.

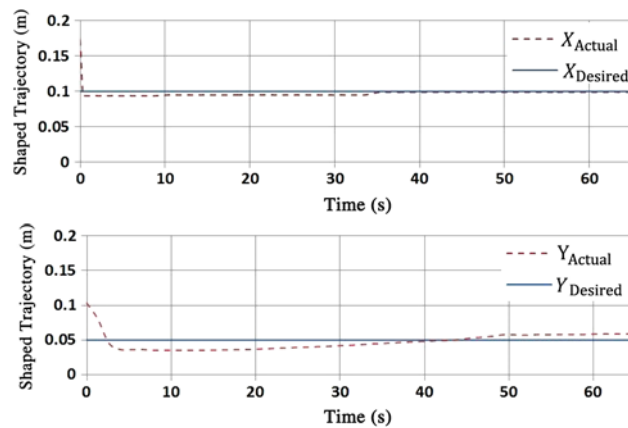


Fig. 15. Position of the shape system and X_S^d .

X and Y . The desired positions of the shape system have been reached during a short time. We find that the relative position between the two slaves following the target trajectory with grasping the object has been achieved. This is in agreement with the experimental result shown in Fig. 15.

8. Conclusion

A novel comprehensive control framework was proposed for the SMMS teleoperation robotic system. The simulation and practical results revealed that the human operator can teleoperate the overall behavior of the multiple slave robots and the grasped object under the control framework which

ensures a secure and tight cooperative grasping among the slave robots regardless of the time-varying communication delay and the human command. To deal with the nonlinearity in the dynamics of the telemanipulators, the uncertainty in the dynamics of the slave robots, and the time-varying delay in the communication channel, two control methodologies were successfully studied, simulated, and tested for the master and the cooperative sides. First, a synchronization control methodology was developed for the master system. Second, two HOSMCs in order to remove chattering effect caused by classical SMC were designed for the shape and the locked systems. The simulation and practical results also revealed that the control framework works well against all of them. Eventually, the closed-loop stability in the presence of the time-varying communication delay and convergence of the tracking errors were proved after defining a particular Lyapunov function using Barbalet's lemma.

References

1. V. Chawda and M. K. O'Malley, "Position synchronization in bilateral teleoperation under time-varying communication delays," *IEEE/ASME Trans. Mechatron.* **20**(1), 245–253 (2015).
2. D. A. Lawrence, "Stability and transparency in bilateral teleoperation," *IEEE Trans. Rob. Autom.* **9**(5), 624–637 (1993).
3. J. T. Wen and K. Kreutz-Delgado, "Motion and force control of multiple robotic manipulators," *Automatica* **28**(4), 729–743 (1992).
4. R. Tinós, M. H. Terra and J. Y. Ishihara, "Motion and force control of cooperative robotic manipulators with passive joints," *IEEE Trans. Control Syst. Technol.* **14**(4), 725–734 (2006).
5. R. Mohajerpoor, M. Rezaei, A. Talebi, M. Noorhosseini and R. Monfaredi, "A robust adaptive hybrid force/position control scheme of two planar manipulators handling an unknown object interacting with an environment," *Proc. Inst. Mech. Eng. Part I: J. Syst. Control Eng.* **226**(4), 509–522 (2012).
6. S. A. Schneider and R. H. Cannon, "Object impedance control for cooperative manipulation: Theory and experimental results," *IEEE Trans. Rob. Autom.* **8**(3), 383–394 (1992).
7. D. Lee and M. W. Spong, "Bilateral Teleoperation of Multiple Cooperative Robots Over Delayed Communication Networks: Theory," *Proceedings of the 2005 IEEE International Conference on Robotics and Automation, 2005, ICRA 2005* (IEEE, 2005) pp. 360–365.
8. H. Kawasaki, S. Ueki and S. Ito, "Decentralized adaptive coordinated control of multiple robot arms without using a force sensor," *Automatica* **42**(3), 481–488 (2006).
9. Y.-H. Liu and S. Arimoto, "Decentralized adaptive and nonadaptive position/force controllers for redundant manipulators in cooperations," *Int. J. Rob. Res.* **17**(3), 232–247 (1998).
10. D. Lee, O. Martinez-Palafox and M. W. Spong, "Bilateral Teleoperation of Multiple Cooperative Robots Over Delayed Communication Networks: Application," *Proceedings of the 2005 IEEE International Conference on Robotics and Automation, 2005, ICRA 2005* (IEEE, 2005) pp. 366–371.
11. R. Monfaredi, S. M. Rezaei and H. A. Talebi, "A Cooperative Robotic System for Handling a Geometrically Unknown Object for Non-rigid Contact Without Force Sensors," *2011 IEEE International Conference on Robotics and Biomimetics (ROBIO)* (IEEE, 2011) pp. 240–245.
12. M. Bistooni and R. Monfaredi, "Cooperative robotic system control scheme for 6DOF spatial handling of a geometrically unknown object," *Trans. Control Mech. Syst.* **3**(2), 93–99 (2014).
13. D. Lee and K. Y. Lui, "Passive configuration decomposition and passivity-based control of nonholonomic mechanical systems," *IEEE Trans. Rob.* **33**(2), 281–297 (2017).
14. M. Kim and D. Lee, "Improving transparency of virtual coupling for haptic interaction with human force observer," *Robotica* **35**(2), 354–369 (2017).
15. K. Y. Lui, H. Cho, C. Ha and D. Lee, "First-person view semi-autonomous teleoperation of cooperative wheeled mobile robots with visuo-haptic feedback," *Int. J. Rob. Res.* **36**(5–7), 840–860 (2017).
16. R. Mohajerpoor, I. Sharifi, H. A. Talebi and S. M. Rezaei, "Adaptive Bilateral Teleoperation of an Unknown Object Handled by Multiple Robots Under Unknown Communication Delay," *IEEE/ASME International Conference on Advanced Intelligent Mechatronics (AIM), 2013* (IEEE, 2013) pp. 1158–1163.
17. Z. Li and C.-Y. Su, "Neural-adaptive control of single-master multiple-slaves teleoperation for coordinated multiple mobile manipulators with time-varying communication delays and input uncertainties," *IEEE Trans. Neural Netw. Learn. Syst.* **24**(9), 1400–1413 (2013).
18. J. Yan, X. Yang, C. Chen, X. Luo and X. Guan, "Bilateral teleoperation of multiple agents with formation control," *IEEE/CAA J. Autom. Sin.* **1**(2), 141–148 (2014).
19. E. J. Rodriguez-Seda, J. J. Troy, C. A. Erignac, P. Murray, D. M. Stipanovic and M. W. Spong, "Bilateral teleoperation of multiple mobile agents: Coordinated motion and collision avoidance," *IEEE Trans. Control Syst. Technol.* **18**(4), 984–992 (2010).
20. Y. Zhang, G. Song, Z. Wei, H. Sun and Y. Zhang, "Bilateral teleoperation of a group of mobile robots for cooperative tasks," *Intell. Serv. Rob.* **9**(4), 311–321 (2016).
21. J. Pliego-Jiménez and M. Arteaga-Pérez, "Telemanipulation of cooperative robots: A case of study," *Int. J. Control.* **91**(6), 1–16 (2017).
22. M. U. Asad, U. Farooq, J. Gu, R. Liu, V. E. Balas and B. Marius, "State Convergence Based Design of a Single-Master-Multi-slave Nonlinear Teleoperation System," *2018 IEEE 14th International Conference on Control and Automation (ICCA)* (IEEE, 2018) pp. 186–191.

23. X. Yang, C.-C. Hua, J. Yan and X.-P. Guan, "Adaptive formation control of cooperative teleoperators with intermittent communications," *IEEE Trans. Cybern.* **99**, 1–10 (2018).
24. E. Nuño, R. Ortega and L. Basañez, "An adaptive controller for nonlinear teleoperators," *Automatica* **46**(1), 155–159 (2010).
25. A. Bartoszewicz and R. J. Patton, "Sliding mode control," *Int. J. Adapt. Control Signal Process.* **21**(8–9), 635–637 (2007).
26. M. W. Spong, S. Hutchinson and M. Vidyasagar, *Robot Modeling and Control*, vol. 3 (Wiley, New York, 2006).
27. T. Hatanaka, N. Chopra, M. Fujita and M. W. Spong, *Passivity-Based Control and Estimation in Networked Robotics* (Springer, Switzerland, 2015).
28. D. Lee, "Passive Decomposition and Control of Interactive Mechanical Systems Under Motion Coordination Requirements," *Ph.D. Dissertation* (University of Minnesota, 2004).
29. G. Bartolini, A. Ferrara, E. Usai and V. I. Utkin, "On multi-input chattering-free second-order sliding mode control," *IEEE Trans. Autom. Control* **45**(9), 1711–1717 (2000).
30. X. Yuhua, Z. Chongwei, B. Wei and T. Lin, "Dynamic Sliding Mode Controller Based on Particle Swarm Optimization for Mobile Robot's Path Following," *International Forum on Information Technology and Applications, IFITA 2009*, vol. 1 (IEEE, 2009) pp. 257–260.
31. S. Ganjefar, F. Janabi-Sharifi, S. Hosseinipناه and R. Sharifi, "Prediction of Delay Time in Internet by Neural Network," *Proceedings of 2005 IEEE Conference on Control Applications, CCA 2005* (IEEE, 2005) pp. 340–345.